Final Technical Report
DE-SC0006642
In Situ Correlated Molecular Imaging of Chemically Communicating Microbial Communities

P.W. Bohn and J.D. Shrout, University of Notre Dame, J.V. Sweedler and S. Farrand, University of Illinois at Urbana-Champaign

I. Overview

This project was organized at the outset around measurement system and biological system goals with the over-arching objective to develop a biological system that closely mimics the rhizosphere and that supports detailed exploration by correlated vibrational (Raman) spectroscopy and mass spectrometry. Specifically, we targeted studies of a three-component system involving two model microorganisms. The bacterium *Pseudomonas aeruginosa* was chosen as a model species for its well-documented surface behavior phenotypes and the possibility of imaging abundant elements of the secretome. While the importance of *P. aeruginosa* signaling molecules (including homoserine lactones and quinolones/quinolones) and surface active compounds (including rhamnolipids) to many *P. aeruginosa* laboratory phenotypes is established, the roles and abundance of such molecules *in situ* has not been characterized. In addition, *P. aeruginosa* is known to remodel its environment by the excretion of a characteristic family of glycolipids, the rhamnolipids, which exhibit characteristic vibrational and mass spectrometric signatures ideal for the development of correlated MS/vibrational imaging tools and allowing the results of the imaging experiments to be interpreted in the context of a complex multi-organism system. Because *P. aeruginosa* is amenable to several genetic techniques, isogenic mutants deficient in production of many of these biomolecular classes could be examined to inform our analyses. While this model system was used initially, we quickly initiated collaborations with investigators at Oak Ridge National Laboratory (ORNL) focused on a 3-component system consisting of multi-kingdom organized communities surrounding the model root derived from *Populus deltoides*, a system that became the target for the latter stages of the project. Thus, our work centered initially around *P. aeruginosa* with the later addition of experiments using a three component system involving *P. deltoides*.

A significant effort involved the creation of technical enhancements and sampling approaches to allow us to advance heterocorrelated mass spectrometry imaging (MSI) and correlated Raman microscopy (CRM) from bacterial cultures and biofilms. We then exploited these measurement advances in heterocorrelated MS/CRM imaging to determine relationship of signaling molecules and excreted signaling molecules produced by *P. aeruginosa* to conditions relevant to the rhizosphere. In particular, we: (1) developed a laboratory testbed mimic for the rhizosphere to enable microbial growth on slides under controlled conditions; (2) integrated specific measurements of (*a*) rhamnolipids, (*b*) quinolone/quinolones, and (*c*) phenazines specific to *P. aeruginosa*; and (3) utilized the imaging tools to probe how messenger secretion, quorum sensing and swarming behavior are correlated with behavior. Our initial hypothesis was that the ectomycorrhyzal environment elicits a distinct “signature profile” that can be discerned from the characteristics of the spatial and temporal properties of the molecular profiles, as discerned by a combination of confocal Raman microscopy (CRM) and mass spectrometric imaging (MSI).

These model system aims were pursued by focusing on (*a*) biofilm growth and development, (*b*) characterization of prominent elements of the molecular secretome in *Pseudomonas aeruginosa* as a function of growth conditions and times, and (*c*) co-cultures of *Pseudomonas* with plants and with other bacteria. Specific advances made in support of these overall objectives are summarized below. References are indexed to the list of DOE-supported publications in **Section IV**.

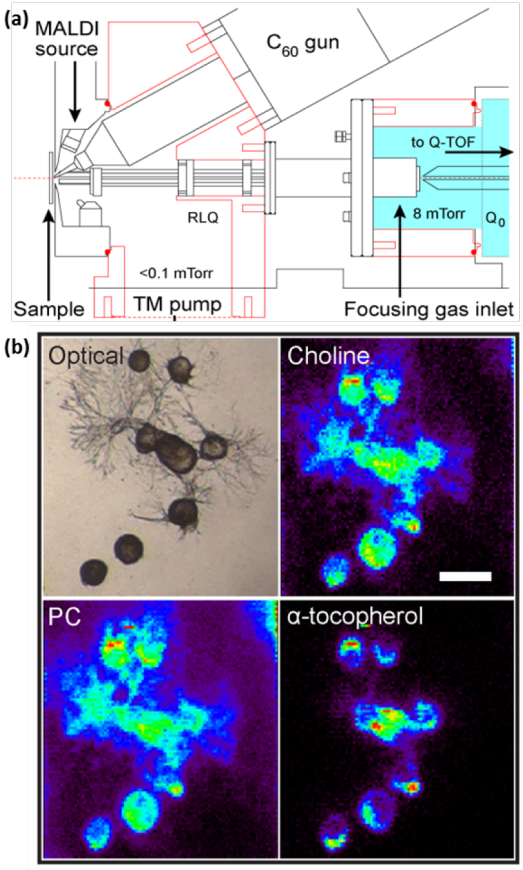

Figure 1. (**a**) Schematic of the source chamber of the hybrid imaging mass spectrometer, (**b**) C_{60}-SIMS images of choline (*m/z* 104.11) the phosphocholine headgroup (*m/z* 184.08) and α-tocopherol (*m/z* 439.39) across an *A. californica* cultured neural network. Adapted from Lanni, E.J., *et al. J. Am. Soc. Mass Spectrom.* **2014,** 25, 1897-1907.

II. Principal Results

II.A. Instrument Design.

Previously limited by intense molecular fragmentation, biomolecular SIMS has been substantially improved by the introduction of polyatomic and cluster primary ion sources. These projectiles—which include C_{60}^+, Ar_n^+, and $(H_20)_n^+$ among others—produce a softer form of ionization then their monatomic counterparts, and therefore enable analysis of larger molecules. The expanded molecular coverage is accompanied by an increase in complexity, as each mass spectrum is effectively a direct infusion, with many isomeric and isobaric compounds presenting with the same effective *m/z* value. To take advantage of the benefits of a cluster ion source and overcome the challenges associated with isobaric interference, we designed and constructed a hybrid spatially resolved MALDI/C_{60}-SIMS Q-ToF mass spectrometer, **Figure 1**(**a**), which is equipped with both a 20 kV C_{60}^+ primary ion beam (1 µm spot size) for SIMS, and a UV-laser for MALDI. The instrument is capable of a mass resolution better than 13,000 FWHM, has a mass range extending to m/z 2000, and has tandem-MS (MS^2) capabilities for *in situ* ion identification. We first demonstrated the imaging capabilities of the spatially resolved mass spectrometer by mapping subcellular metabolite distributions across cultured neural networks from the California sea hare *Aplysia californica*, **Figure 1(b)**.

In addition to facilitating *in-situ* molecular identification, the MS^2 capabilities of this instrument allow for product ion imaging, in which a tandem mass spectrum is acquired for every point within a region of interest. Product ion imaging provides a highly specific distribution of a given

analyte, as the ion can be distinguished and mapped based upon both the *m/z* value of the precursor ion and the presence of molecular-specific fragments. We first applied SIMS product ion imaging to differentiate two isomers—*i.e.* 2-nonyl-3-hydroxy-4-quinolone (C9-PQS) and 2-nonyl-4-quinoline-*N*-oxide (NQNO)—in early-growth biofilms of *P. aeruginosa*, **Figure 2**. With the overwhelming majority of the intense product ions resulting from NQNO, this result revealed the *N*-oxide isomer as the dominant molecular species found at m/z 288.21 in agreement with the initial assignment based on the CRM principal component analysis (PCA).[13]

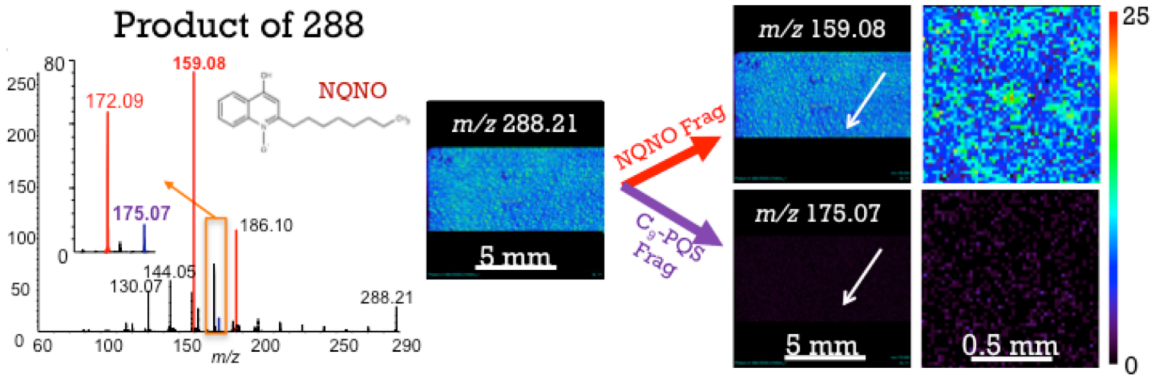

Figure 2. C_{60}-SIMS product ion imaging of *m/z* 288.2 in 7-hr *P. aeruginosa* biofilms reveals the distribution of the isomeric pair, 2-nonyl-4-quinoline-*N*-oxide (NQNO, red fragments) and 2-nonyl-3-hydroxy-4-quinolone (C9-PQS, blue fragments). The ion images show *m/z* 159.08 (specific to NQNO) to be distributed in a series of high abundance spots across the sample surface. Adapted from [13].

II.B. Ionization Enhancement for C_{60}-SIMS.

While polyatomic and cluster ion sources have extended the usable mass range for SIMS, fundamental constraints on the availability of biomolecules caps the obtainable lateral resolution to about 1 μm. Improvements beyond this threshold require innovative strategies to increase ionization efficiency. We have taken two sample preparation approaches that were originally developed for other ionization modalities and adapted them for use with C_{60}-SIMS. We found that sublimation of 0.1–0.2 mg cm^{-2} layer of 2,5-dihydrobenzoic acid (DHB) onto mammalian nervous system tissue provided significant enhancement for glycerophospholipid ions.[8]

In a second study specifically orientated toward bacterial biofilms, we used the hybrid imaging mass spectrometer described in **Section II.A** to examine the effects of a thin gold coating for improving ionization in both C_{60}-SIMS and LDI. By imaging the same sample with a microprobe spot that is smaller than the space between rows, the same unperturbed sample was examined with SIMS and LDI before and after gold coating. A combination of qualitative image comparison, multivariate analysis, and quantitative intensity profiling showed that sputtering the sample surface with a few-nm layer of gold improves ionization for a diverse set of biomolecules including 2-alkyl-4-quinolones and rhamnolipids, two of the critical secretome classes described in **Section I**. The metallization was also found to significantly reduce fragmentation and subsequent ionization of background ions from the culture medium, resulting in spectra that are generally cleaner and of higher quality.[15]

Remarkably, metallized samples can be analyzed with a diverse collection of imaging methods, as the same metal coating is agreeable with LDI, monatomic SIMS, and electron microscopy. Taking advantage of this broad utility, we developed a correlated imaging approach that begins with LDI of a gold coated sample to generate a broad molecular map for subsequent analysis

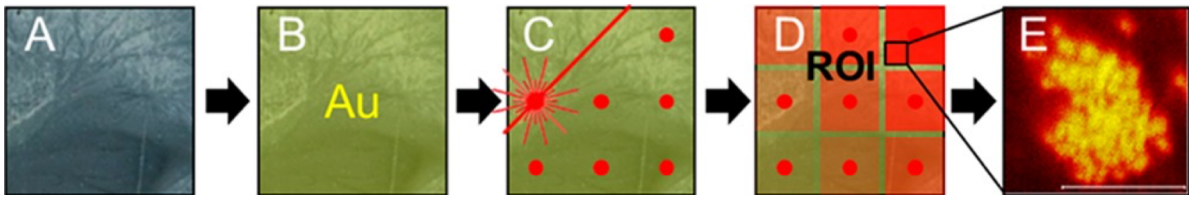

Figure 3. Workflow schematic of a MALDI-guided SIMS experiment, illustrating: (**a**) sample preparation to meet vacuum MS requirements (must be flat, dry, and mounted to a conducting or semiconducting substrate), (**b**) surface chemical treatment for ion signal enhancement, (**c**) undersampling MALDI MS image acquisition across the specimen surface, (**d**) specification of ROIs for SIMS analysis based on the MALDI chemical map, and (**e**) SIMS imaging at microscopic ROIs. Adapted from [9].

with high-resolution monatomic SIMS.[9] By performing step-mode LDI at a large spot offset a region between the ablation craters (which act as fiducial marks) is left unperturbed for SIMS imaging (**Figure 3**).

(3) Nanoparticle Enabled Correlated Imaging.

While the utility of biomolecular SIMS, and more broadly MSI as a whole, is indisputable, the technique remains encumbered by several limitations. The sample preparation can be arduous, matrix effects preclude routine quantification, and it is primarily a high vacuum technique—which necessitates sample preservation steps that impede multiple observations of the same unperturbed system. Molecular identification can also be challenging, because each pixel is effectively a direct injection, with multiple analytes presenting with the same or nearly the same

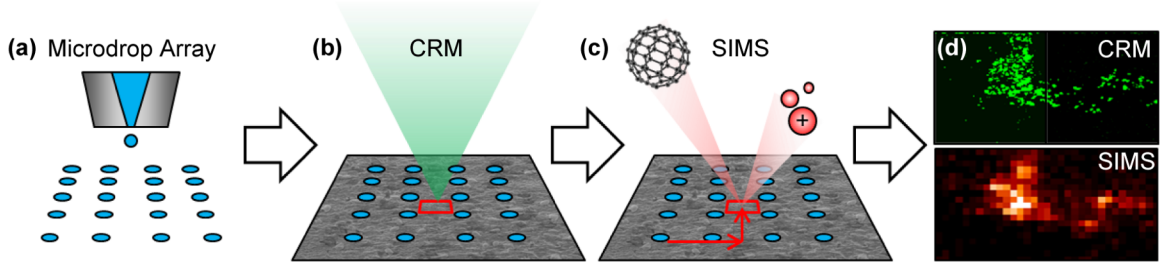

Figure 4. CRM/SIMS correlated imaging workflow. (**a**) A microdroplet array is applied to the dried biofilm. (**b**) CRM is performed to locate ROIs and array coordinates are recorded. (**c**) The sample is transferred to the SIMS instrument and the array is used to navigate back to the ROIs. (**d**) The CRM and SIMS data are correlated, using the array for alignment. Adapted from [10].

m/z value. For these reasons we have sought to correlate MSI with different imaging modalities, especially CRM, which can be performed on live samples and offers a second route for molecular identification, and scanning electron microscopy, which provides structural

morphological information.

Because of the large range of spatial dimensions examined (sub-μm to several-cm), correlating these three imaging modalities is particularly challenging, especially when the approach is applied to examine a sample, such as a bacterial biofilm, with no macroscopic landmarks that can be used to register spatial locations between imaging platforms. To overcome these challenges we developed a nanoparticle-based correlated imaging procedure in which a precisely ordered array of nanoparticle droplets is spotted across the sample surface. The nanoparticle spots provide a fiducial grid and allow the researcher to collect offline information from the same region of interest with several different analytical techniques. We demonstrated this method on biofilms by first imaging different analyte classes with CRM—including proteins, carbohydrates, and quinolones—and imaging the same region with C_{60}-SIMS to assign more precise molecular information (**Figure 4**).[10] Offline SEM provided structural information about the biofilm and the integration of the three techniques showed that quinolone "hotspots" are aligned with regions of exposed cells on the colony surface.

(4) Multimodal Chemical Imaging of *P. aeruginosa* Bacterial Communities

Even without exact spatial registry combining multiple techniques to interrogate the same system

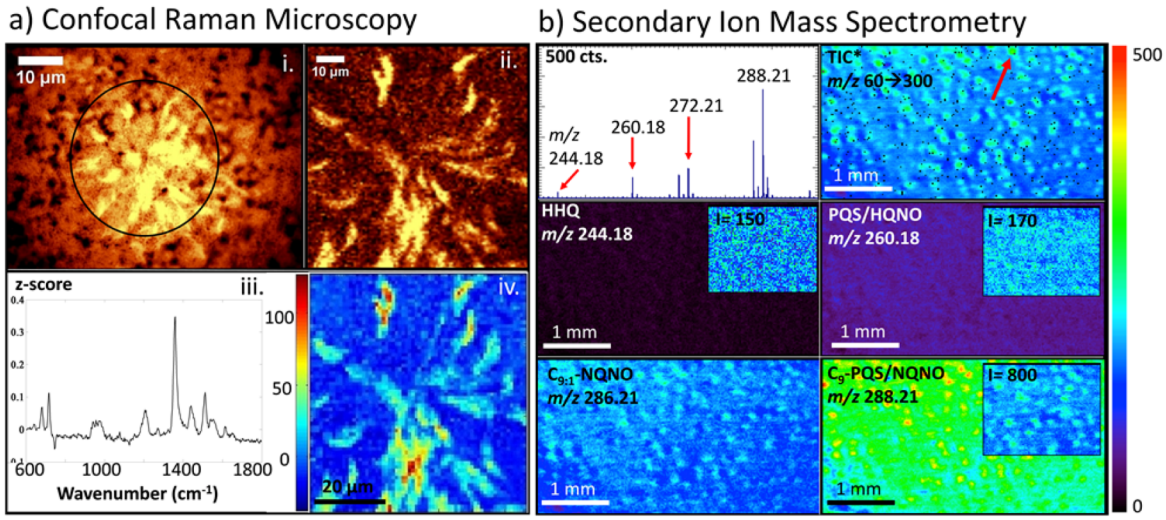

Figure 5. (**a**) Bright field microscopy and CRM, and (**b**) targeted SIMS imaging and microspectroscopy of a 7 h *P. aeruginosa* biofilm. (**a**) (**i**) Bright field microscopy of a quinoline rich region found in 7 h static biofilms; (**ii**) Raman image acquired from the circled region in (**i**) and integrated over 1338–1376 cm^{-1}; (**iii**) PC3 from the Raman image; (**iv**) heat map showing the spatial distribution and magnitude of PC3. (**b**) SIMS imaging of regions of high AQ abundance. Inset regions with variable color map intensity show that patterning is present for most AQs, however the intensity differences are most pronounced for the isomeric C9-PQS/NQNO ion at *m/z* 288.21. The mass spectrum is an average of four pixels from a representative high-intensity region of the TIC image (as indicated by the red arrow). The TIC images include values in the m/z 60–300 range, scaled from 0 to 2 counts, while the individual ion images are scaled as indicated by the color bar on the right. Adapted from [13].

can produce superior information than that which can be obtained from a single technique in isolation. In a series of studies, [6,10,13] we have used the combined analytical capabilities of CRM, MSI and SEM to investigate the spatiochemical composition and architectural features of *P. aeruginosa* biofilms. In the first study, we applied CRM to show that in contrast to planktonic cells, three-day old wild-type biofilms are largely composed of glycolipids, polysaccharides and secreted proteins. LDI-MS revealed rhamnolipids as the primary glycolipid species present in this model system. A similar CRM/MSI comparison of the wild-type phenotype and a mutant strain incapable of producing rhamnolipids and quorum sensing molecules (Δ*lasI*Δ*rhlI*) showed that the two phenotypes are similar in the planktonic state, but drastically different when they form biofilms. This analysis also suggested that biofilms cannot form in the absence of rhamnolipids and quorum sensing molecules.[6]

In a separate study we applied our multimodal imaging strategy to study 2-alkyl-4-quinolones/quinoline-*N*-oxides (AQs) during the formation of *P. aeruginosa* biofilms. The combination of C_{60}-SIMS and CRM showed that *N*-oxide AQs, which are known for their involvement in defending the colony from gram-positive bacteria, are highly abundant during the onset of biofilm development. The N-oxide AQs share the same *m/z* value with other compounds—most notably molecules from the "*Pseudomonas* quinolone signal" (PQS) class—and are therefore very difficult to image with MS alone. Raman scattering, on the other hand produces highly characteristic, easily distinguishable Raman patterns. Our investigations here also showed that the *N*-oxide AQs form clumps on the biofilm surface, possible providing further insight into their functional role in biofilm biology (**Figure 5**).[13]

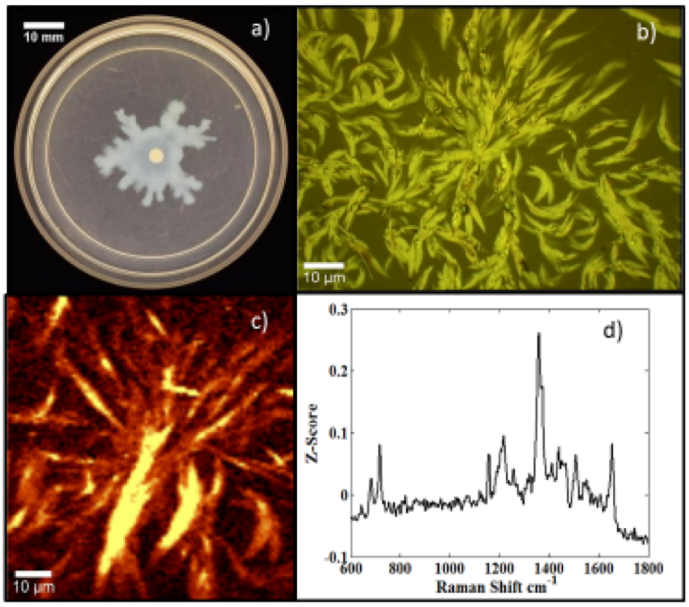

Figure 6. (a) Image of a *P. aeruginosa* swarm zone, (b) bright field microscopy of quinolone rich regions within the swarm zone, (c) Raman image acquired from the quinolone rich region pictured in (b) in a 48 h swarm plate constructed from a 1338–1376 cm^{-1} filter to include the marker band for quinolones/quinolines; (d) loading plot of PC1 generated from analysis of the Raman image of the 48 h swarm plate. PC1 contains features that correspond to bands from both PQS and HQNO standard spectra. Adapted from [13].

Further, we also employed CRM imaging for non-destructive, *in situ* characterization of AQ signaling molecules and secondary metabolites in swarm motility zones of *P. aeruginosa* (**Figure 6**). To our knowledge *in situ* analysis of the chemical dynamics of swarm zones of *P. aeruginosa* with molecular imaging techniques has not been previously reported. Our investigations reveal that quinolones/quinolines tend to accumulate in regions of the swarm zone where the bacteria have presumambly colonized the surface

and have started forming biofilms, as opposed to the very edges of the swarm zones which are primarily comprised of actively motile cells. These observations provide an insight into the dichotomy between swarming motility and biofilm formation.[13]

III. Conclusions and Key Findings

Correlated chemical imaging is an emerging strategy for acquisition of images by combining information from multiplexed measurement platforms to track, visualize, and interpret *in situ* changes in the structure, organization, and activities of interesting chemical systems, such as multi-component microbial communities, that frequently span multiple decades in space and time. Acquiring and correlating information from complementary imaging experiments, such as CRM and MSI, has the potential to expose complex chemical behavior in ways that are simply not available from single methods applied in isolation. However, in order to accurately correlate image information across platforms, a number of issues must be addressed: (1) signals obtained from disparate experiments exhibit fundamentally different figures of merit, including pixel size, spatial resolution, dynamic range, and acquisition rates; (2) images are often acquired on different instruments in different locations, requiring spatial registration of the sample, so that the same area of the sample landscape is addressed; (3) signals acquired must be correlated in both spatial and temporal domains; and (4) the resulting information has to be presented in a way that is readily understood. These requirements pose special challenges for image cross-correlation that go well beyond those posed in single technique imaging approaches.

The work carried out under DOE support in this project has produced advances in two areas: development of new highly sophisticated correlated imaging approaches and the application of these new tools to the growth and differentiation of microbial communities under a variety of environmental conditions. The major findings and conclusions are summarized below.

III.A. Analytical Technique Development

1. We developed a sequentially combined chemical imaging approach wherein an undersampled MALDI MS image is used to guide microscopic SIMS imaging experiments. This combination exhibits numerous advantages for MSI, including: (1) specifying microscopic ROIs from a chemical map rather than an optical image; (2) spatially registered macro- and microscopic chemical images of a single sample; (3) generation of a fiducial grid for sample navigation in SIMS; and (4) MALDI MS/MS capability for *in situ* ion characterization. In biofilms of *P. aeruginosa*, MALDI-guided SIMS enabled detection and visualization of secondary metabolites, including rhamnolipid surfactants and quinolone signaling molecules that had not been reported using SIMS alone. The combination of SIMS and MALDI revealed both macroscopic and cell-scale chemical heterogeneity across the biofilms for the analytes studied, and can be applied to other samples where similar multi-scale complexity exists, such as tissue sections.[9]

2. We reported a method that combines two label-free molecular imaging techniques, CRM and MSI, using a chemical microspot array printed on the sample to allow precise navigation, re-location of analysis regions, and alignment of correlated image data. CRM enabled nondestructive imaging with sub-μm spatial resolution of secreted quinolones and detection of multiple biomolecule classes. MSI with C_{60}-SIMS allowed mass-based discrimination of

multiple specific quinolone species having subtly differing distributions, as well as confirmation of mass assignments with *in situ* MS/MS experiments. SEM images showed that quinolone concentrations detected with SIMS and resolved by CRM correlate with single cells exposed on the biofilm surface, demonstrating that the CRM-MSI imaging approach serves as an effective platform for *in situ* single cell metabolomics.[10]

3. We compared the small molecule imaging capabilities of metal-assisted C_{60}-SIMS (MetA-C_{60}-SIMS) to both C_{60}-SIMS and MetA-LDI, and demonstrated that MetA-C_{60}-SIMS is viable for small molecule imaging of complex biological systems. Sputtering the biofilm surface with an effective 2.5 nm layer of gold increased sensitivity and improved spectral purity through reduced ionization of background ions. Metallization improved C_{60}-SIMS ionization in biofilms for several molecular classes, including 2-alkyl-4-quinolones and RHLs, by up to 300%. MetA-SIMS ionization relies upon the interplay between the chemical and physical properties of both the sample and the analytes themselves.[16]

III.B. Microbial Community Development

1. CRM and MSI were combined to characterize chemical composition and structure in *P. aeruginosa* – both planktonic cells and biofilms in both the wild type and in a quorum sensing mutant strain (Δ*las*Δ*rhlI*) incapable of producing either rhamnolipids or the homo-serine lactones used in quorum sensing. Wild type planktonic cells exhibit spectra that are dominated by DNA/RNA-related spectral features – bands that are absent in the biofilm. Instead, biofilms produce spectra that are dominated by rhamnolipids and by a co-secreted protein/peptide component. In contrast, the quorum sensing mutant exhibits very similar spectra to the planktonic cells after 72 h. These observations indicate the formation of a thick biofilm after 72 h in the wild type cells, but not in the quorum sensing-deficient mutant. MALDI MS profiling was applied to obtain more chemically specific information on the variety of rhamnolipids present; nine putative rhamnolipid species were detected in the wild-type biofilm, six of which could be confirmed by tandem MS.[6]

2. Combined SIMS and CRM imaging was used to characterize the spatial distribution of several quinolone quorum sensing molecules and quinoline secondary metabolites across the surface of *P. aeruginosa* in various states of organization. CRM in conjunction with PCA was first used to identify broad molecular classes, *e.g.* quinolones and quinolines, and this information was used to guide mass spectrometric analysis. This multimodal approach indicated that the primary AQs belong to the N-oxide family as opposed to the isomeric PQS family at 7-h of biofilm growth. In contrast 48-h biofilms are marked by a dramatic decrease in the quantity of all AQs and a shift from the N-oxide family towards the PQS family, with co-localization of the two species. These combined CRM/MSI experiments demonstrated the acquisition of molecular information across length scales from a few μm to cm. These results suggest an important role for N-oxide quinolines in early biofilm formation and show that the transition from the planktonic state to the formation of a biofilm is marked by a dramatic increase in the presence of the N-oxide family of quinolines, and chemical similarities between swarming motility and early biofilms indicate conserved chemical expression across multiple phenotypes.[13]

IV. Publications

The following publications acknowledge support of grant DE-SC0006642.

[1] Nie, B.; Duan, B.; Bohn, P.W., Silver-Coated Porous GaN Nanostructures for Laser Induced Desorption/Ionization Mass Spectrometry. *ACS Appl. Mater. Interf* **2012,** 5, 6208-6215.

[2] Nie, B.; Masyuko, R.; Bohn, P.W., Correlation of Surface-enhanced Raman Spectroscopy and Laser Desorption-Ionization Mass Spectrometry Acquired from Silver Nanoparticle Substrates. *Analyst* **2012,** 137, 1421-1427.

[3] Barnhart, D.M.; Su, S.; Baccaro, B.E.; Banta, L.M.; Farrand, S.K., CelR, an Ortholog of the Diguanylate Cyclase PleD of Caulobacter, Regulates Cellulose Synthesis in Agrobacterium tumefaciens. *Appl. Environ. Microbiol.* **2013,** 79, 7188-7202.

[4] Masyuko, R.; Lanni, E.; Sweedler, J.V.; Bohn, P.W., Correlated Imaging - A Grand Challenge in Chemical Analysis. *Analyst* **2013,** 138, 1924-1939.

[5] Rubakhin, S.S.; Lanni, E.J.; Sweedler, J.V., Progress Toward Single Cell Metabolomics. *Curr. Opin. Biotechnol.* **2013,** 24, 95-104.

[6] Masyuko, R.; Lanni, E.; Driscoll, C.M.; Shrout, J.D.; Sweedler, J.V.; Bohn, P.W., Spatial Organization of Pseudomonas Aeruginosa Biofilms Probed by Correlated Laser Desorption Ionization Mass Spectrometry and Confocal Raman Microscopy. *Analyst* **2014,** 139, 5700-5708.

[7] Barnhart, D.M.; Su, S.; Farrand, S.K., A Signaling Pathway Involving the Diguanylate Cyclase CelR and the Response Regulator DivK Controls Cellulose Synthesis in Agrobacterium tumefaciens. *J. Bacteriol.* **2014,** 196, 1257-1274.

[8] Lanni, E.J.; Dunham, S.J.B.; Nemes, P.; Rubakhin, S.S.; Sweedler, J.V., Biomolecular Imaging with a C60-SIMS/MALDI Dual Ion Source Hybrid Mass Spectrometer: Instrumentation, Matrix Enhancement, and Single Cell Analysis. *J. Am. Soc. Mass Spectrom.* **2014,** 25, 1897-1907.

[9] Lanni, E.J.; Masyuko, R.N.; Driscoll, C.M.; Aerts, J.T.; Shrout, J.D.; Bohn, P.W.; Sweedler, J.V., MALDI-guided SIMS: Multiscale Imaging of Metabolites in Bacterial Biofilm. *Analyt. Chem.* **2014,** 85, 9139-9145.

[10] Lanni, E.J.; Masyuko, R.N.; Driscoll, C.M.; Aerts, J.T.; Shrout, J.D.; Bohn, P.W.; Sweedler, J.V., Correlated Imaging with C60-SIMS and Confocal Raman Microscopy: Visualization of Cell-Scale Molecular Distributions in a Bacterial Biofilm. *Analyt. Chem.* **2014,** 85, 10885-10891.

[11] Shaw, K.; Contento, N.M.; Xu , W.; Bohn , P.W., Nanofluidic Structures for Coupled

Sensing and Remediation of Toxins. *Proc. SPIE – Smart Biomedical and Physiological Sensor Technology XI* **2014,** 9107, 91070L.

[12] Wetzel, M.E.; Kim, K.-S.; Miller, M.; Olsen, G.J.; Farrand, S.K., Quorum-Dependent Mannopine-Inducible Conjugative Transfer of an Agrobacterium Opine-Catabolic Plasmid. *J. Bacteriol.* **2014,** 196, 1031-1044.

[13] Baig, N.F.; Dunham, S.J.B.; Morales-Soto, N.; Shrout, J.D.; Sweedler, J.V.; Bohn, P.W., Multimodal Chemical Imaging of Molecular Messengers in Emerging Pseudomonas aeruginosa Bacterial Communities. *Analyst* **2015,** 140, 6544-6552.

[14] Wetzel, M.E.; Olsen, G.J.; Chakravartty, V.; Farrand, S.K., The repABC Plasmids with Quorum-Regulated Transfer Systems in Members of the Rhizobiales Divide into Two Structurally and Separately Evolving Groups. *Genome biology and evolution* **2015,** 7, 3337-3357.

[15] Dunham, S.J.B.; Comi, T.J.; Ko, K.; Li, B.; Baig, N.F.; Morales-Soto, N.; Shrout, J.D.; Bohn, P.W.; Sweedler, J.V., Metal-assisted polyatomic SIMS and LDI for enhanced small molecule imaging of bacterial biofilms. *Biointerphases* **2016**, submitted.